OPEN

Citation: Oncogenesis (2013) **2**, e47; doi:10.1038/oncsis.2013.10

www.nature.com/oncsis

ORIGINAL ARTICLE

Overexpression of miR-26a-2 in human liposarcoma is correlated with poor patient survival

DH Lee[1,2], S Amanat[1], C Goff[1], LM Weiss[3], JW Said[2], NB Doan[2], A Sato-Otsubo[4], S Ogawa[4], C Forscher[1] and HP Koeffler[1,5]

Approximately 90% of well-differentiated/de-differentiated liposarcomas (WDLPS/DDLPS), the most common LPS subtype, have chromosomal amplification at 12q13-q22. Many protein-coding genes in the region, such as *MDM2* and , have been studied as potential therapeutic targets for LPS treatment, with minimal success. In the amplified region near the *MDM2* gene, our single nucleotide polymorphism (SNP) array analysis of 75 LPS samples identified frequent amplification of miR-26a-2. Besides being in the amplicon, miR-26a-2 was overexpressed significantly in WDLPS/DDLPS ($P<0.001$), as well as in myxoid/round cell LPS (MRC) ($P<0.05$). Furthermore, Kaplan–Meier survival analysis showed that overexpression of miR-26a-2 significantly correlated with poor patient survival in both types of LPS ($P<0.05$ for WDLPS/DDLPS; $P<0.001$ for MRC). Based on these findings, we hypothesized that miR-26a-2 has an important role in LPS tumorigenesis, regardless of LPS subtypes. Overexpression of miR-26a-2 in three LPS cell lines (SW872, LPS141 and LP6) enhanced the growth and survival of these cells, including faster cell proliferation and migration, enhanced clonogenicity, suppressed adipocyte differentiation and/or resistance to apoptosis. Inhibition of miR-26a-2 in LPS cells using anti-miR-26a-2 resulted in the opposite responses. To explain further the effect of miR-26a-2 overexpression in LPS cells, we performed *in silico* analysis and identified 93 candidate targets of miR-26a-2. Among these genes, *RCBTB1* (regulator of chromosome condensation and BTB domain-containing protein 1) is located at 13q12.3-q14.3, a region of recurrent loss of heterozygosity (LOH) in LPS. Indeed, either overexpression or inhibition of RCBTB1 made LPS cells more susceptible or resistant to apoptosis, respectively. In conclusion, our study for the first time reveals the contribution of miR-26a-2 to LPS tumorigenesis, partly through inhibiting RCBTB1, suggesting that miR-26a-2 is a novel therapeutic target for human LPS.

Oncogenesis (2013) **2,** e47; doi:10.1038/oncsis.2013.10; published online 20 May 2013

Subject Categories: molecular oncology

Keywords: liposarcoma; SNP array; microRNA; survival; RCBTB1; apoptosis

INTRODUCTION

Human liposarcoma (LPS) is the most common soft-tissue sarcoma, comprising 24–45% of the total soft-tissue sarcomas.[1,2] Surgical resection can effectively manage primary local disease, but metastatic disease cannot be cured either by surgery, chemotherapy or radiotherapy. Despite its high occurrence, the molecular causes of this sarcoma are poorly understood. LPS is grouped in three major subtypes depending on their histopathological characteristics:[1,2] (1) Well-differentiated/de-differentiated (WDLPS/DDLPS), (2) myxoid/round cell LPS (MRC) and (3) pleomorphic LPS. WDLPS/DDLPS is the most common subtype and is characterized by chromosomal amplification at 12q13-q22, which contains the *MDM2* and *CDK4* genes in 90% of the cases. Laboratory investigators have focused on blocking the function of these amplified genes with Nutlin 3a and several novel compounds, respectively.[1–4] To date, these approaches have shown disappointing clinical outcomes.

For a better understanding of LPS, we performed genome-wide copy number (CN) analysis of 75 human LPS samples, using single nucleotide polymorphism (SNP) array. Our preliminary study found that miR-26a-2 is amplified and highly expressed in LPS. MicroRNA (miRNA) is a short, non-coding RNA that can regulate the expression of multiple target genes in a cell-type-specific manner.[5] miRNAs classically interact with the 3′-untranslated region (UTR) region of the target mRNAs, resulting in the degradation of the mRNA and/or the inhibition of translation of the target gene. Changes in the expression of miRNAs often occur with malignant transformation. For example, 11% of glioblastoma multiforme (GBM) have amplification and overexpression of the miR-26a-2.[6,7] This miRNA is known to target the tumor-suppressor genes *PTEN* and *RB1*.[6,7] Therefore, targeting of dysregulated miRNA is an appealing new option for cancer therapy.[5]

In this study, we investigated the *in vitro* effect of miR-26a-2 on the proliferation and survival of LPS cells. We also identified a novel, LPS-specific target protein of miR-26a-2 that could partly explain the effect of miR-26a-2 in LPS cells.

RESULTS

Recurrent genomic aberrations in human LPS

Characteristics of 72 human LPS patients, whose DNA was subjected to SNP array analysis, are summarized in Table 1. More than half of the tumor specimens were WDLPS/DDLPS (43 samples, 57% of all the samples), followed by MRC (22 samples, 29%). Only three samples represented pleomorphic LPS. The samples were from 39 males (52% of the patients) and 29

[1]Division of Hematology and Oncology, Cedars-Sinai Medical Center, UCLA School of Medicine, Los Angeles, CA, USA; [2]Department of Pathology and Laboratory Medicine, Santa Monica-University of California-Los Angeles Medical Center, Los Angeles, CA, USA; [3]Department of Pathology, City of Hope, Duarte, CA, USA; [4]Cancer Genomics Project, Graduate School of Medicine, University of Tokyo, Tokyo, Japan and [5]National Cancer Institute and Cancer Science Institute, National University of Singapore, Singapore, Singapore. Correspondence: Dr DH Lee, Division of Hematology and Oncology, Cedars-Sinai Medical Center, UCLA School of Medicine, 8700 Beverly Boulevard, D5022, Los Angeles, CA 90048, USA.
E-mail: hiromasa@ucla.edu
Received 31 January 2013; revised 1 April 2013; accepted 9 April 2013

females (39%). Average age of the patients was 57 ± 15 years, ranging from 14 to 86 years. Median follow-up period was 36 months.

SNP array analysis identified 6107 total CN) changes, including those successfully identified recurrent genomic changes previously reported (Table 2).[8] The most distinct feature of the CN changes in LPS was the dominance of CN gains over CN losses. Nearly 91% of the CN changes were CN gains (total 5532 CN gains). Many of these CN gains were identified on chromosome 12 (1968 gains), especially at chromosome 12q13-q22 (757 gains) (Figures 1a and b). Sixty-six percent of the samples showed various levels of CN gain in the region (48 samples). When we considered only WDLPS/DDLPS, the percentage of CN gains surged to 83% (35 samples). Other recurrent regions of CN gain were also identified (Table 2). Recurrent CN gain at 1q21-q24 occured in 40% of the samples (29 samples), followed by 5p13-p15 (24 samples, 33%) and 6q22-q24 (23 samples, 32%).

Close examination of CN gain in 12q13-q22 identified two distinct amplicons, MDM2 amplicon (A_1) and miR-26a-2 amplicon (A_2), which were almost always present in the samples with 12q amplification (Figure 1a). The miR-26a-2 amplicon, also commonly known as CDK4 amplicon,[9] showed a strong correlation with the appearance of the MDM2 amplicon. Among 41 samples with a miR-26a-2 amplicon (mostly WDLPS/DDLPS), 36 of these samples had an accompanied MDM2 amplicon (85%) (Table 3). Likewise, among 28 samples without a miR-26a-2 amplicon (mostly MRC), 26 samples also did not have a MDM2 amplicon (93%). A χ^2 test proved that the occurrence of these two amplicons are not independent, but are strongly correlated ($P < 0.001$).

In addition to total CN changes, SNP array analysis revealed recurrent regions of loss of heterozygosity (LOH) in LPS (Figures 1c–e). LOH occurs by either deletion alone, or deletion of one allele followed by duplication of the other allele (CN-neutral LOH). Genes in the LOH region often have important roles in cancer biology and are frequently mutated.[10] This is especially the case with CN-neutral LOH where one normal allele is lost, and the other allele is mutated and then duplicated.

A total of 575 events (9%) of LOH by deletion occurred in the 75 LPS samples (Table 2). LOH by deletion at 13q12.3-a14.3 was the most frequent change (9 samples, 12%), with a homozygous deletion in some of those cases (Supplementary Table S1). Regarding CN-neutral LOH, a total of 110 events occured in 23 LPS samples (Supplementary Table S2). Nearly half of the CN-neutral LOH (50 events, 45%) were found in only three samples (LPS19, LPS44 and LPS63). The most recurrent region of CN-neutral LOH was Xp22.33-p21.1 (six events), followed by 2q31.1, 12p11.22-q12, 13q12.3-q14.3, 14q12, 17q11.1-q11.2 and Xq26.2-qter (all five events). Overall, the 13q12.3-q14.3 region showed the highest LOH frequency in LPS.

Table 1. Characteristics of 72 patients, whose LPS samples were studied. Total number of patients $n = 72$

Characteristics	*Value*
Age	
Mean ± s.d.	57 ± 15 Years
Range	14 ~ 86 Years
Gender	
Male	39 (52%)
Female	29 (39%)
Unknown	4 (9%)
Histologic subtype	
WD	28 (37%)
DD	15 (20%)
MRC	22 (29%)
P	3 (4%)
Mixed/NOS	4 (9%)
Median follow-up	36 Months

Abbreviations: DD, dedifferentiated LPS; LOH, loss of heterozygosity; MRC, myxoid/round cell LPS; NOS, not otherwise specified; P, pleomorphic LPS; WD, well-differentiated LPS.

Overexpression of miR-26a-2 and its correlation with poor patient survival

CN gains of the miR-26a-2 amplicon identified by SNP array were validated by genomic quantitative PCR (qPCR) (Figure 2a). The median CN of the miR-26a-2 gene was significantly higher than that of the non-matched normal fat tissues in WDLPS/DDLPS

Table 2. Recurrent genomic changes in human liposarcomas (LPS)

Cytoband	*WD* (n = *28*)	*DD* (n = *15*)	*MRC* (n = *22*)	P (n = *3*)	*NOS* (n = *5*)	*Total* (n = *73*)
CN gain						
12q13-q22	22 (79%)	14 (93%)	7 (32%)	1	4	48 (66%)
1q21-24	14 (50%)	6 (40%)	6 (27%)	2	1	29 (40%)
5p13-p15	6 (21%)	11 (73%)	4 (18%)	1	2	24 (33%)
6q22-q24	9 (32%)	6 (40%)	4 (18%)	2	2	23 (32%)
CN loss						
13q12.13-q14.3	4 (14%)	1 (7%)	2 (9%)	1	1	9 (12%)
CN-neutral LOH						
Xp22.32-p21.1	2 (7%)	2 (13%)	2 (9%)	0	0	6(8%)
2q31.1	2 (7%)	2 (13%)	0 (0%)	1	0	5 (7%)
12p11.22-q12	1 (4%)	1 (7%)	1 (5%)	1	1	5 (7%)
13q12.3-q14.3	2 (7%)	1 (7%)	1 (5%)	1	0	5 (7%)
14q12	2 (7%)	1 (7%)	1 (5%)	1	0	5 (7%)
17q11.1-q11.2	1 (4%)	1 (7%)	1 (5%)	1	1	5 (7%)
Xq26.2-qter	1 (4%)	2 (13%)	2 (9%)	0	0	5 (7%)

Abbreviations: CN, copy number; DD, dedifferentiated LPS; LOH, loss of heterozygosity; MRC, myxoid/round cell LPS; NOS, not otherwise specified; P, pleomorphic LPS; WD, well-differentiated LPS.

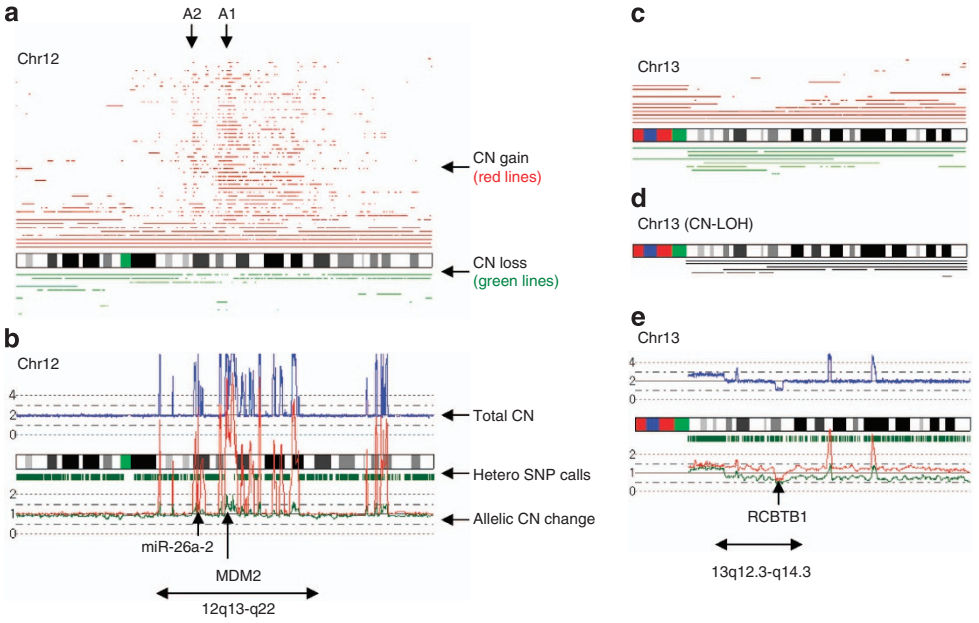

Figure 1. Recurrent genomic changes in human LPS. SNP array results of 75 LPS samples. Two representative genomic changes in human LPS at 12q13-q22 (panels **a** and **b**) and at 13q12.3-q14.3 (panels **b**–**e**) are shown. (**a**) Integral view of chromosome 12 demonstrates recurrent CN gains of 12q13-q22 (red). Each bar indicates the region of CN changes in each sample. Two of the most recurrent amplicons are shown: Amplicon A_1 is centered on *MDM2* gene. Amplicon A_2 contains miR-26a-2 gene. (**b**) CNAG output of chromosome 12 for sample LPS2 is shown as an example. (**c**) Integral view of chromosome 13 showing recurrent LOH by deletion at 13q12.3-q14.3 (green). (**d**) Integral view of chromosome 13 showing recurrent CN-LOH of 13q12.3-q14.3 (black). (**e**) CNAG output of chromosome 12 for sample LPS44 is shown as an example.

Table 3. Status of MDM2 amplicon (amplicon A_1) and miR-26a-2 amplicon (amplicon A_2) as determined by SNP array analysis of 75 human LPS samples

Amplicon	*Frequency*	*WD*	*DD*	*MRC*	P	*NOS*
Amplicon A_1 and A_2	39 (52%)	16	14	6	0	3
Amplicon A_1 only	5 (7%)	4	0	0	1	0
Amplicon A_2 only	2 (3%)	1	0	1	0	0
No amplicon	26 (35%)	6	1	14	2	3
Unknown	3 (4%)	1	0	1	0	1
Total	75 (101%)					

Abbreviations: DD, dedifferentiated LPS; LOH, loss of heterozygosity; MRC, myxoid/round cell LPS; NOS, not otherwise specified; P, pleomorphic LPS; WD, well-differentiated LPS.

($P<0.001$) and MRC ($P<0.05$). DDLPS showed the highest median CN gain, followed by WDLPS and MRC (Figure 2b).

Overexpression of miR-26a-2 gene was identified by Quantitative reverse-transcription real-time PCR (qRT-PCR) (Figures 2c and d). The significant increase in the median expression level was found in DDLPS ($P<0.001$) and MRC ($P<0.001$), but not in WDLPS ($P=0.415$), although some WDLPS samples did show high expression of the gene. The expression level of the miR-26a-2 gene, however, was not always CN-driven. In DDLPS, expression level of miR-26a gene strongly correlated with the CN status of the gene, with a Pearson's correlation coefficient (R) of 0.53. In contrast, WDLPS showed no significant increase of miR-26a-2 expression level, although a significant increase of the median CN gain of miR-26a-2 gene occurred ($R=0.16$). Furthermore, MRC showed a significantly increased expression of the miR-26a-2 gene even though this group had the lowest median CN gain of the miR-26a-2 gene ($R=0.21$). Overall, overexpression of miR-26a-2 gene was seen in the majority of the samples, but the CN-driven overexpression occured only in DDLPS.

We examined the correlation of miR-26a-2 expression level to known clinical parameters. First, we performed paired analysis of five LPS samples and their matched normal fat tissues (Figure 3a). Three out of five samples (LPS12, LPS19 and LPS22) showed significantly increased expression level of the miR-26a-2 compared with levels of the gene in matched normal fat tissue ($P<0.05$ for all). Individuals from these three LPS samples had a worse prognosis than the other two individuals (LPS11 and LPS13) without significant changes in the miR-26a-2 expression level compared with matched normal fat control. Therefore, we expanded the analysis to all samples with patient survival data.

Kaplan–Meier survival analysis was performed on 17 patients with WD/DDLPS and 22 individuals with MRC. Patients whose tumors had higher miR-26a-2 expression level had a worse prognosis in both the WD/DDLPS ($P<0.05$) and MRC cohorts ($P<0.001$) (Figures 3b and c). Other clinical parameters such as age and gender did not show any significant correlation with the levels of miR-26a-2 (data not shown).

Effect of miR-26a-2 on growth and survival of LPS cells

To examine the function of miR-26a-2 in LPS cells, we used three LPS cell lines, SW872, LPS141 and LP6, which showed low, medium and high endogenous expression of miR-26a-2, respectively (Supplementary Figure S1A). For each cell line, we established stable overexpression clones of miR-26a-2 (Supplementary Figure S1B). Overexpression of miR-26a-2 in these LPS cells stimulated the growth and survival of LPS cells with varied outcomes (Supplementary Figures S1C–F).

We also examined the effect of inhibition of miR-26a-2 using anti-miR-26a-2 oligos. SW872 cells were excluded due to their minimal endogenous expression of miR-26a-2. Anti-miR-26a-2 oligos successfully inhibited the expression of miR-26a-2 by around 50% in both LPS141 and LP6 cells (Supplementary Figure S1G). Decreased miR-26a-2 levels inhibited the growth and survival of LPS cells with varied outcomes (Supplementary Figures S1H-K).

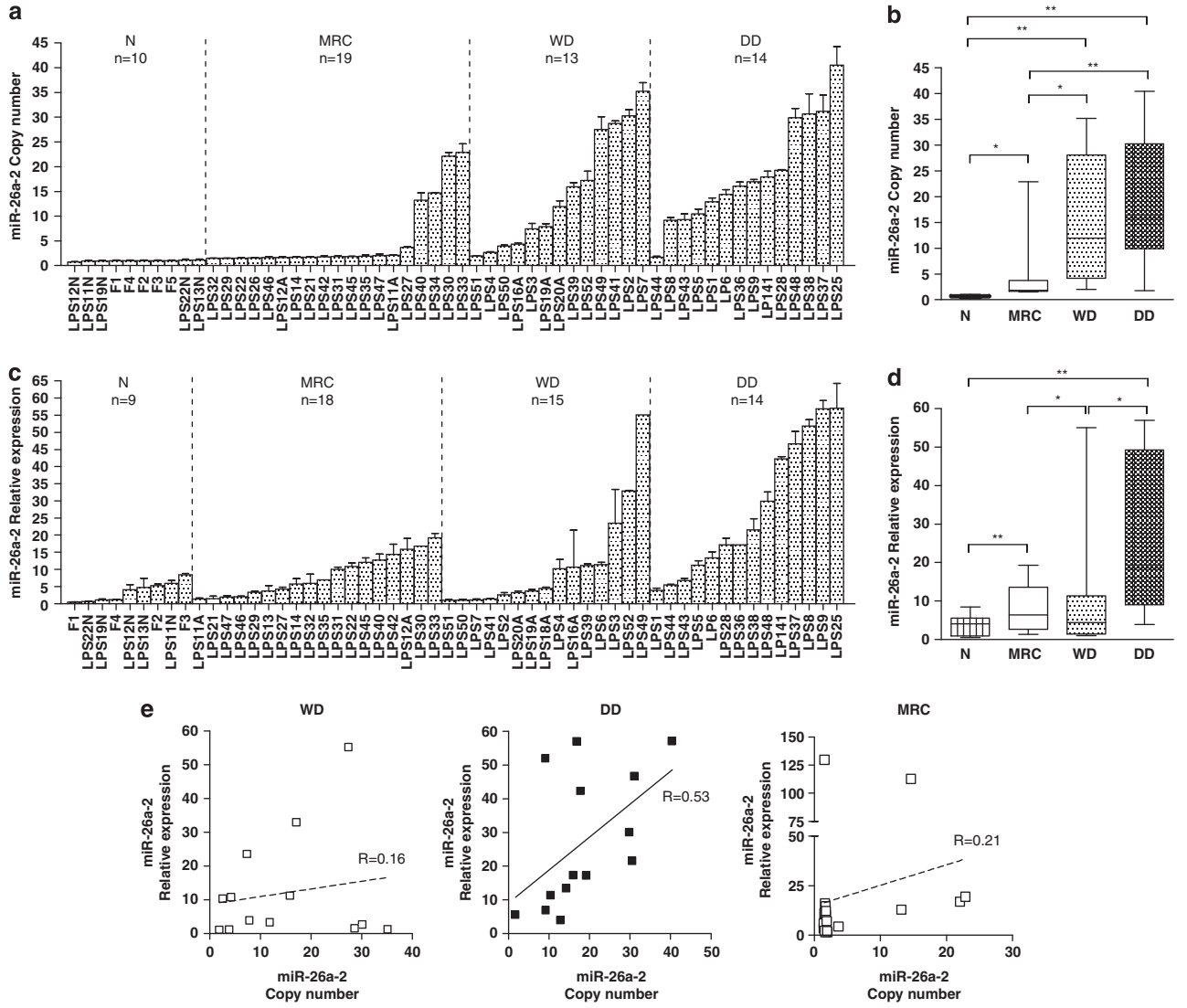

Figure 2. Changes in CN status and RNA expression level of miR-26a-2 gene in human LPS samples. (**a**) CN of miR-26a-2 gene in LPS determined by genomic qPCR. CN changes relative to the CN of normal human adipose tissue samples (*N*) are shown. Samples are grouped by LPS subtype: MRC = myxoid/round cell subtype; WD = well-differentiated subtype; DD = dedifferentiated subtype; n = sample number. Experiments were repeated in triplicates to ensure accuracy. Data represent mean CN ± s.d. (**b**) Box-whisker plot showing summary of data in panel (**a**). Asterisks (* and **) indicate *P*-values <0.05 and 0.001 by *t*-test, respectively. (**c**) RNA expression level of miR-26a-2 gene determined by qRT-PCR. Expression levels relative to the expression level in normal human adipose tissue samples are shown. Data represent mean RNA expression ± s.d. (**d**) Box-whisker plot showing summary of data in panel (**c**). (**e**) Pearson's correlation study of the CN change and mRNA expression level of miR-26a-2 gene. *R* represents Pearson's correlation coefficient. *R* value >0.5 is considered significant.

Modulation of miR-26a-2 expression also affected genes important for adipocyte differentiation. SW872 and LP6 clones with overexpression of miR-26a-2 showed significant inhibition of mRNA expression of these genes ($P<0.05$) (Figures 4a and b). Western blot results also showed a modest downregulation of expression of C/EBPα and C/EBPβ proteins in the SW872 and LP6 cells, respectively. Inhibition of miR-26a-2 using anti-miR-26a-2 did not change the mRNA expression level of these genes (data not shown), but caused upregulation C/EBPα, C/EBPβ and PPARγ proteins in the LPS141 and LP6 cells, as noted on western blot (Figure 4c). Despite the clear changes in the differentiation marker genes, forced differentiation of the clones using differentiation media did not induce terminal differentiation, indicating a block in this pathway (data not shown).

Interestingly, modulation of miR-26a-2 in the LPS cells affected their resistance to apoptotic stress. miR-26a-2 overexpression clones of SW872 and LP6 cells had 41 ± 3 and $59 \pm 4\%$ apoptosis, respectively, after apoptotic stress compared to 51 ± 5 and $67 \pm 7\%$ of the empty vector control cells, respectively ($P<0.05$ for both) (Figure 4d). The same experiments were repeated except that miR-26a-2 was inhibited by using anti-miR-26a-2 oligonucleotides (Figure 4e). After exposure to apoptotic stress, $28 \pm 4\%$ of LPS141 cells treated with anti-miR-26a-2 oligos became apoptotic, compared with $23 \pm 3\%$ of cells treated with scrambled oligo control ($P<0.05$). Likewise, $27 \pm 2\%$ of the LP6 cells treated with anti-miR-26a-2 oligo became apoptotic, compared with $20 \pm 2\%$ of cells treated with scrambled oligos control ($P<0.05$).

Identification of target proteins of miR-26a-2 in LPS

PTEN and RB1 are well-known tumor-suppressor genes as well as known targets of miR-26a-2.[6,7] In LPS cells, we could not find evidence that either PTEN or RB1 was regulated by miR-26a-2 (Supplementary Figure S2). Both PTEN and RB1 did not change,

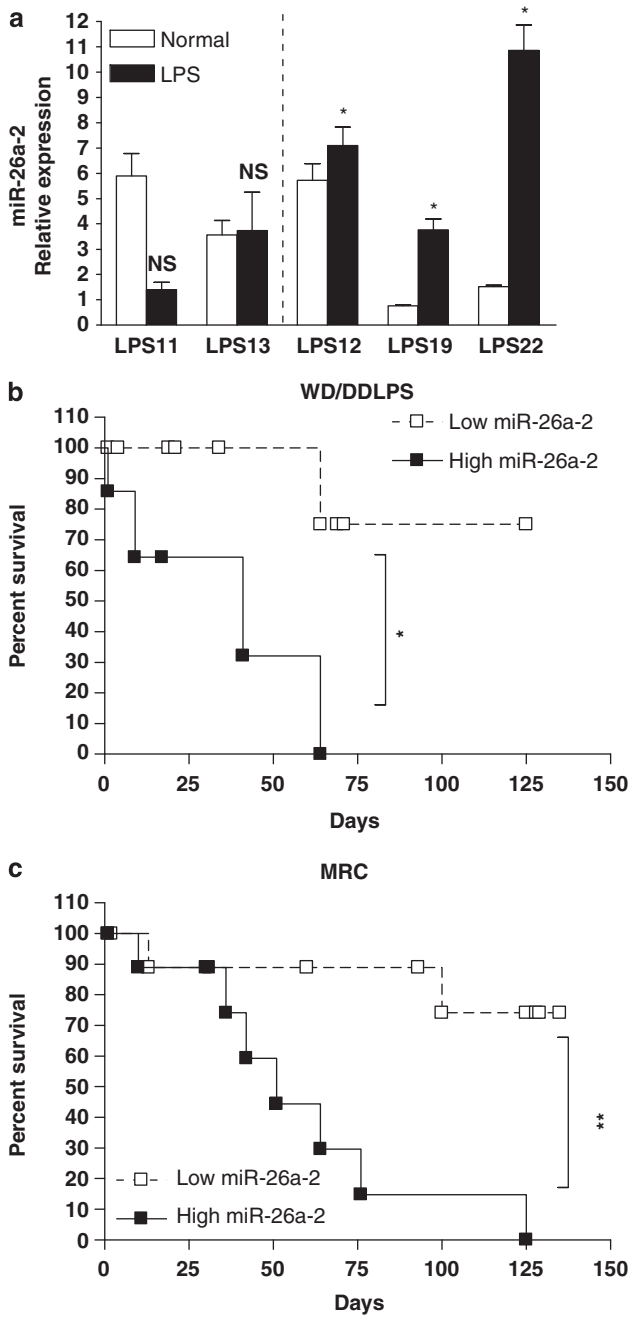

Figure 3. Correlation between miR-26a-2 expression and patient survival. (**a**) Paired analysis of LPS samples with matched normals. Five LPS samples with matched normals were analyzed for the correlation of miR-26a-2 expression and its relationship to patient survival (Supplementary Table S4). Each bar represents average relative expression ± s.d. Asterisk (*) indicates *P*-value <0.05 by *t*-test. NS = not significant. (**b**) Kaplan–Meier survival analysis of LPS patients. Patients were divided into two groups according to their miR-26a expression level, using the data in Figure 2c. Median expression fold change (10-fold) was used as a cutoff value. (low, $<$10-fold increase in miR-26a-2 expression; high, $\geqslant$10-fold). Asterisks (**) indicate *P*-value <0.001 by log-rank test. WD/DD = well-differentiated/dedifferentiated LPS subtype; MRC = myxoid/round cell LPS subtype.

compared with the control cells in the presence of forced expression of miR-26a-2 or anti-miR-26a-2 in LPS cells. Likewise, the phosphorylation status of Akt at S473, a PTEN target, did not change as U87 GBM cells did in response to the changes in miR-26a-2 level.

This led us to search for new targets of miR-26a in LPS cells. We performed *in silico* analysis to identify putative miR-26a-2-binding sites using five miRNA target-prediction webservers.[11–15] Ninety-three candidate genes were selected which were predicted as targets of miR-26a-2 by more than three webservers (Supplementary Table S3). The list successfully included all known targets of miR-26a-2 gene, such as *PTEN* and *RB1*. Comparison of this list with our SNP array data suggested that RCBTB1 (regulator of chromosome condensation and BTB domain-containing protein 1) at 13q12.3-q14.3, a recurrent region of LOH in LPS cells, may be a putative target of miR-26a-2 in LPS. In addition, homozygous deletion of RCBTB1 in one of our primary LPS tumor samples (LPS44, Supplementary Table S1) also suggested that LPS cells want to lower or eliminate the expression of this gene.

Dual luciferase reporter assay confirmed that miR-26a-2 could bind to the putative binding site in the RCBTB1 3′-UTR and achieved a $\sim$50% knockdown of the luciferase gene (Figures 5a and b). Point mutations at the miR-26a-2-binding site partially restored the luciferase activity to the level of empty vector control, indicating that the binding was site-specific.

To validate further that RCBTB1 is regulated by miR-26a-2 in LPS cells, we examined if RCBTB1 responded to the changes in miR-26a-2 expression level. RCBTB1 is known as a regulator of the DNA damage/repair pathway and apoptosis.[16] Under apoptotic stress, RCBTB1 and its downstream target GADD45α (growth arrest and DNA-damage-inducible protein α) are known to be upregulated.[16] Under apoptotic stress, the level of upregulation of RCBTB1 and GADD45α in miR-26a-2 overexpression clones of SW872 and LP6 cells was lower than that of the similarly stimulated empty vector control cells (Figure 5c). Likewise, under the same culture conditions, the level of upregulation of RCBTB1 and GADD45α in LPS141 and LP6 cells transfected with anti-miR-26a-2 was higher than the level in scrambled oligo control cells (Figure 5d). From these results, we concluded that RCBTB1 is indeed the target of miR-26a-2 in LPS cells.

Role of RCBTB1 in LPS cells

As expected, overexpression of RCBTB1 made LPS cells more susceptible to apoptotic stress (Figures 6a–c). Expression of RCBTB1 alone increased the number of apoptotic cells from 8 ± 1 to $26 \pm 3\%$ in LPS141 cells, and from 6 ± 1 to $24 \pm 3\%$ in LP6 cells ($P<0.05$). With apoptotic stress, the increase was even more apparent. The number of apoptotic cells under apoptotic stress increased from 42 ± 5 to $71 \pm 7\%$ in LPS141 cells, and from 47 ± 3 to $77 \pm 10\%$ in LP6 cells ($P<0.05$).

We also established stable clones of SW872 and LPS141 cells expressing short hairpin RNA (shRNA) against RCBTB1, which significantly decreased the levels of RCBTB1 (Figure 6d). Both shRNA clones showed higher resistance to apoptotic stress (Figures 6e and f). Under apoptotic stress, the number of apoptotic cells of the SW872 shRNA clones increased from 3 ± 0.2 to $44 \pm 3\%$ (SH1), and from 5 ± 0.2 to $45 \pm 2\%$ (SH2), compared with 6 ± 0.3 to $50 \pm 3\%$ in the scrambled control cells ($P<0.05$). Likewise, the number of apoptotic cells of LPS141 shRNA clones increase from 2 ± 0.2 to $12 \pm 2\%$ (SH1), and from 3 ± 0.1 to $16 \pm 4\%$ (SH2), compared with the change from 5 ± 1 to $24 \pm 3\%$ in scrambled control cells ($P<0.05$).

To validate further the inhibition of RCBTB1 by miR-26a-2, we cotransfected the miR-26a-2 and RCBTB1 expression vectors in SW872 cells (Figure 7). We constructed a new RCBTB1 expression vector containing 3′-UTR miR-26a-2-binding site (RCBTB1-3UTR) and compared the results with the one without 3′-UTR (RCBTB1). Cotransfection of miR-26a-2 with RCBTB1-3UTR significantly decreased the number of apoptotic cells from 54 ± 8 to $36 \pm 4\%$ ($P<0.05$). Cotransfection of miR-26a-2 with RCBTB1 also showed a

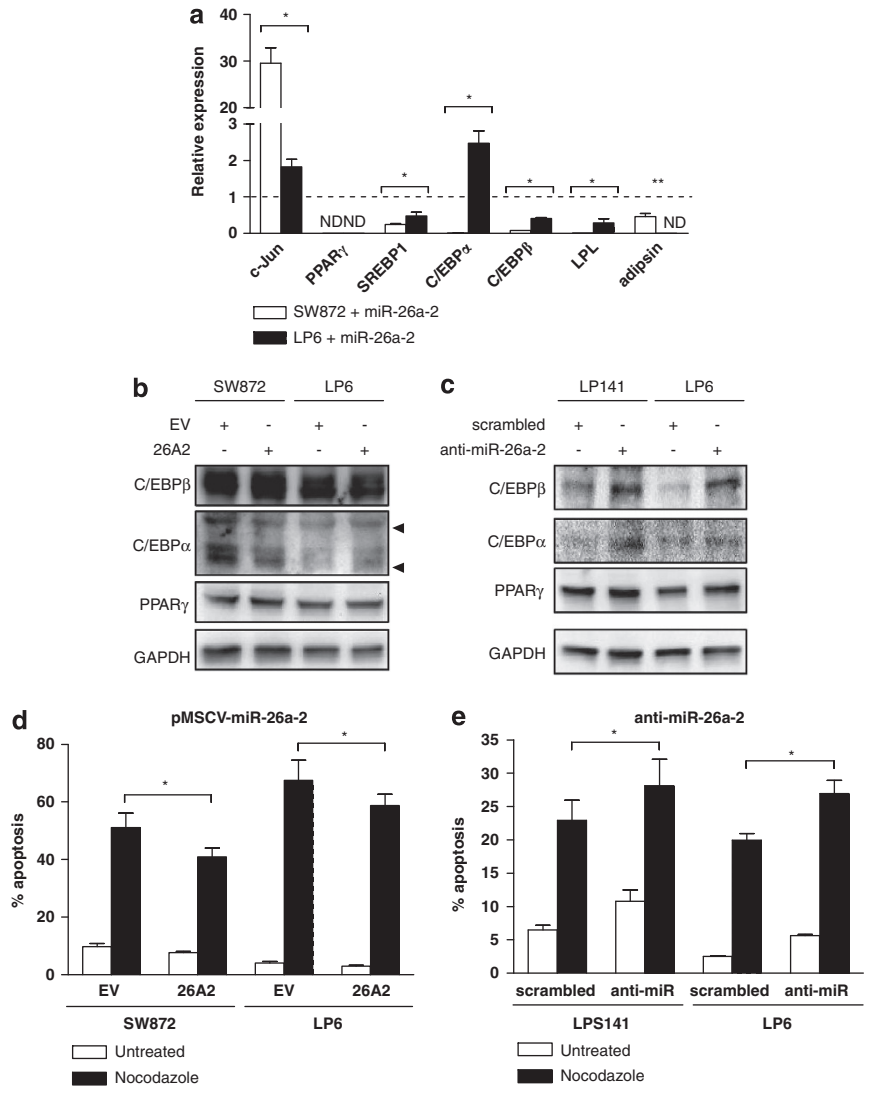

Figure 4. Effect of miR-26a-2 on adipocyte differentiation and apoptosis in LPS cells. For panels (**a**), (**b**) and (**d**), LPS cells were transduced with either pMSCV-miR-26a-2 expression vector (26A2) or empty vector control. Stable clones were selected with puromycin. For panels (**c**) and (**e**), LPS cells were transfected with either scrambled control oligos or anti-miR-26a-2 oligos. Cells were harvested 24 h after transfection. (**a**) mRNA expression level of adipocyte differentiation marker genes in miR-26a-2 overexpression clones. Dashed line indicates the normalized expression level of each gene compared with the empty vector clones. (**b**) Western blots showing protein expression level of C/EBPβ, C/EBPα and PPARγ in miR-26a-2 overexpression clones. GAPDH was used as a loading control. (**c**) Protein expression level of C/EBPβ, C/EBPα and PPARγ in LPS cells transfected with anti-miR-26a-2 oligos. (**d**) Apoptosis assay results of miR-26a-2 overexpression clones after 72 h of exposure to nocodazole. (**e**) Apoptosis assay results of cells transfected with anti-miR-26a-2 after 72 h exposure to nocodazole. Experiments were repeated three times to ensure accuracy. Data represent average ± s.d. (error bars). Asterisks (* and **) indicate *P*-values <0.05 and 0.001 by *t*-test, respectively.

small decrease in the number of apoptotic cells from 68 ± 7 to 58 ± 12%, but was not statistically significant ($P=0.14$). In addition, the inhibitory effect of miR-26a-2 was greater when the apoptosis was induced by RCBTB1-3UTR, rather than RCBTB1 (34 ± 6 versus15 ± 2, $P<0.05$).

DISCUSSION

In this study, we analyzed the genomic aberrations of 75 human LPS and identified several new recurrent regions of genomic abnormalities, most notably the recurrent LOH in 13q12.3-q14.3. This region is well known for the high prevalence of tumor-suppressor genes such as RB1 and miR-15a/16-1, which are frequently mutated or deleted in many cancers.[17] However, its importance in LPS tumorigenesis has not been reported. Our observation can be attributed to the use of SNP array combined with AsCNAR algorithm that can differentiate allele-specific CN changes such as CN-neutral LOH.[18] Indeed, half of the LOHs in 13q12.3-q14.3 were CN-neutral LOH, rather than LOH by deletion. Unlike CN gain at 12q13-q22, which was predominantly found in DDLPS, LOH at 13q12.3-q14.3 was not subtype-specific, indicating that genes in the region contributed to LPS tumorigenesis in a more general way. Recently, Barretina *et al.*[19] reported CN-neutral LOH events in LPS, but did not identify recurrent regions, partly due to the low number of events. Their group also reported somatic mutations in LPS, but none of these genes was located at 13q12.3-q14.3.[19] Extensive exon sequencing of the genes in the region may identify new somatic mutations in LPS.

Interestingly, two of the most recurrent genomic changes in LPS (CN gain in 12q13-q22 and LOH in 13q12.3-q14.3) resemble the recurrent genomic changes in chronic lymphocytic leukemia.

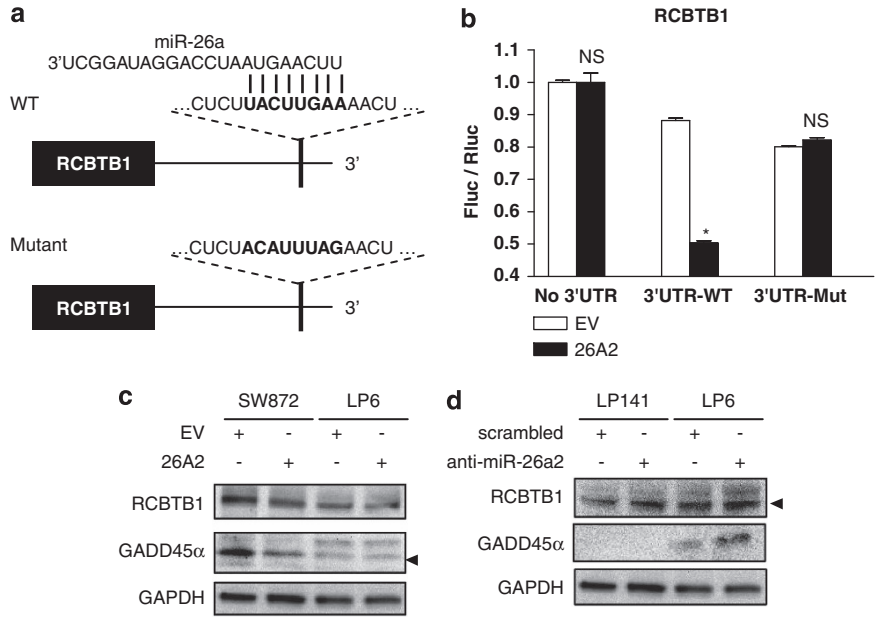

Figure 5. RCBTB1 as a target of miR-26a-2 in LPS cells. (**a**) Schematic diagram of RCBTB1 3′-UTR showing seed sequence (5′-UACUUGAA-3′) of miR-26a-2-binding site. In mutant, seed sequence was mutated to 5′-ACAUUUAG-3′ by site-directed mutagenesis. (**b**) Luciferase assay results. pGL3-Promoter-RCBTB1 3′-UTR luciferase reporter vector was cotransfected with either miR-26a-2 expression vector (26A2) or empty vector control (EV) in 293T cells. After 48 h, cells were harvested and luciferase activity was quantified. Fluc/Rluc = Firefly luciferase/Renilla luciferase. (**c**) Levels of RCBTB1 and GADD45α in miR-26a-2 overexpression clones (26A2) and EV control clones of SW872 and LP6 cells. Cells were exposed to apoptotic stress (nocodazole) for 48 h before harvesting. GAPDH was used as a loading control. (**d**) Levels of RCBTB1 and GADD45α in LPS141 and LP6 cells treated with either anti-miR-26a-2 oligos or scrambled control oligos. Cells were exposed to apoptotic stress (nocodazole) for 48 h before harvesting. Experiments were repeated three times to ensure accuracy. Data represent average ± s.d. (error bars). Asterisk (*) indicate *P*-value <0.05 by *t*-test. NS, not significant.

Trisomy chromosome 12 or CN loss at 13q12.3-q14.3 often occur in chronic lymphocytic leukemia, and usually occur in a mutually exclusive fashion.[16,20] Our statistical analysis could not identify such a correlation in LPS, but many samples with CN loss at 13q12.3-q14.3 often lacked the CN gain at 12q13-q22 (data not shown). Increasing the sample size may identify a possible correlation between the two genomic changes in LPS.

Among the many genes in the 12q13-q22 region, we focused on the miR-26a-2 gene for several reasons: first, many protein-coding genes in the region have been studied as potential therapeutic targets for LPS treatment, with minimal success to date. Second, the miR-26a-2 amplicon occurred nearly as frequently as the MDM2 amplicon. Third, the oncogenic role of miR-26a-2 in GBM could suggest a similar role for the gene in LPS. Indeed, overexpression of miR-26a-2 enhanced the growth and survival of the LPS cells with varied outcomes. However, the stimulatory pathway engaged by overexpression of miR-26a-2 in LPS cells seems to differ from the mechanism previously reported in GBM cells. In GBM, overexpression of miR-26a-2 directly inhibits the key growth signaling proteins such as PTEN and RB1.[7] In LPS, miR-26a-2 overexpression had little effect on these proteins for unclear reasons. Rather, miR-26a-2 inhibited the key proteins related to adipocyte differentiation and apoptosis, which indirectly promoted the growth and survival of LPS cells. Inhibition of RCBTB1 can partly explain the effect of miR-26a-2 in LPS cells. As a regulator of the DNA damage/repair pathway and apoptosis,[16] inhibition of RCBTB1 by overexpression of miR-26a-2 made LPS cells more resistant to apoptotic stress. However, RCBTB1 had little effect on the differentiation of adipocyte (data not shown), which implies the existence of another major target protein of miR-26a-2 in LPS cells.

Interesting but unexplored is our observation that the primary DDLPS tumor sample (LPS44) with a homozygous deletion of RCBTB1 had no amplification of chromosome 12, which is very unusual in DDLPS. It is one of the samples that we noted, suggesting a possible correlation of CN loss in 13q12.3-q14.3 and the CN gain at 12q13-q22. The diminished expression of RCBTB1 may substitute for the overexpression of miR-26a-2 in LPS cells. Clearly, further studies are needed to examine the significance of this relation.

Next to RCBTB1 is RCBTB2, which is also homozygously deleted in LPS44. Despite their proximity and structural similarity, RCBTB1 and RCBTB2 are paralogs that share little biological function. Unlike RCBTB1, RCBTB2 is not deleted recurrently in chronic lymphocytic leukemia and has no miR-26a-2-binding site in its 3′-UTR region. Therefore, it is unlikely that RCBTB2 has a similar role as RCBTB1 in LPS. However, its interaction with COPS4 (constitutive photomorphogenic homolog subunit 4) suggests that RCBTB2 may have an important role by regulating the phosphorylation of p53 and c-Jun.[21]

In conclusion, our SNP array results contribute to our global molecular characterization of human LPS. The strong association of miR-26a-2 expression level with patient survival suggests the contribution of miR-26a-2 to LPS tumorigenesis. We also identified a new target gene of miR-26a-2, *RCBTB1*. Taken together, new therapeutic targets have been identified for this pernicious cancer.

MATERIALS AND METHODS

Primary human LPS specimens

Seventy-two primary human LPS tumor tissues, as well as clinical data were obtained from various sources with IRB approval from each institution (Supplementary Table S4). Nine LPS samples (LPS1–LPS9, numbers in order of acquisition) were provided by Dr Jonathan Said at the University of California (Los Angeles, CA, USA). Fourteen samples (LPS11–LPS24) were

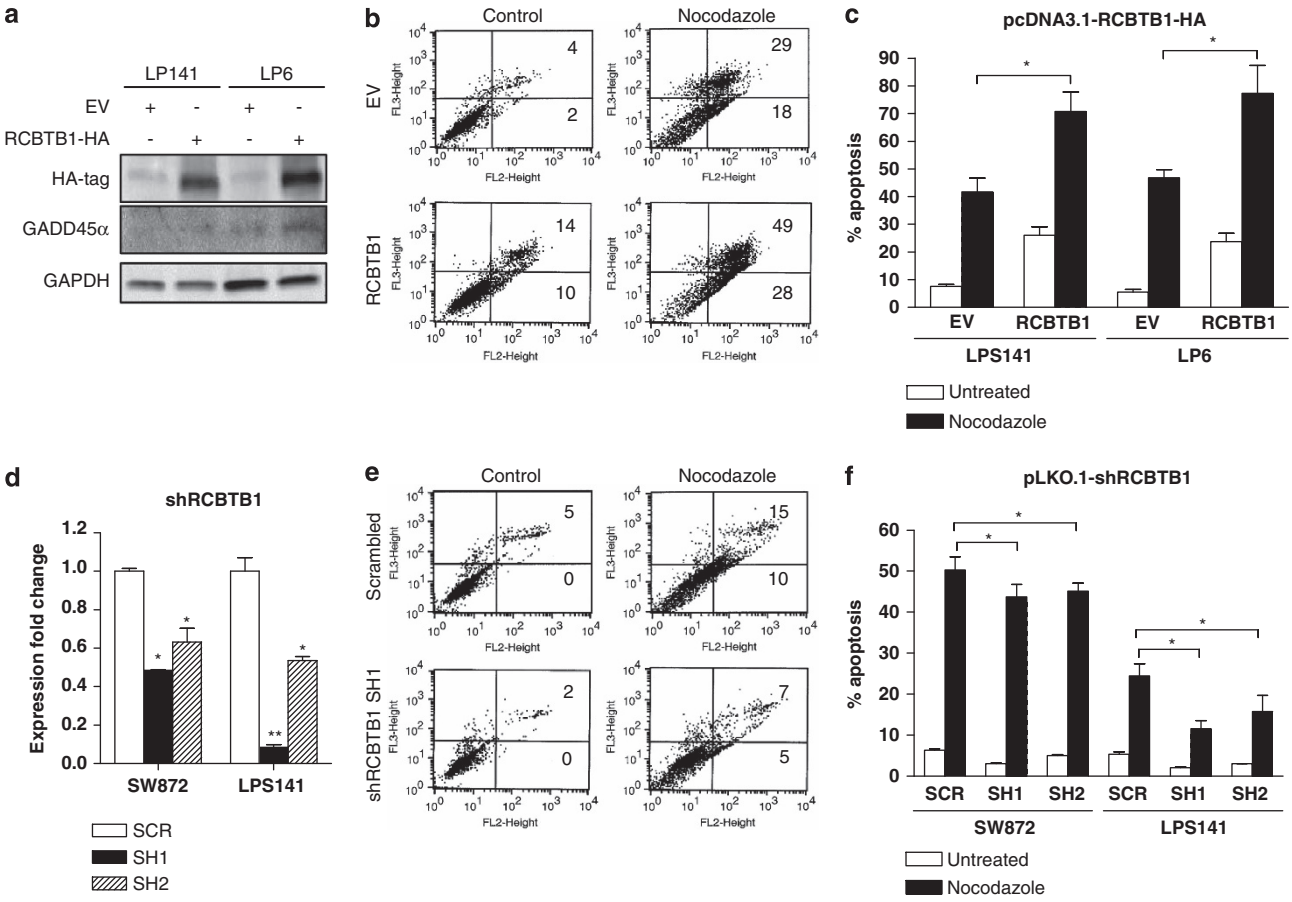

Figure 6. Effect of RCBTB1 on the apoptosis of LPS cells. (**a**) Western blot results showing overexpression of RCBTB1. LPS141 and LP6 cells were transiently transfected with either RCBTB1-HA tag expression vector (RCBTB1-HA) or EV. (**b**) Apoptosis assay results of LP6 cells shown as a representative image. (**c**) Summary of apoptosis assay results. LPS141 and LP6 cells in panel (**a**) were exposed to apoptotic stress (nocodazole) for 48 h, and subjected to FACS analysis. (**d**) qRT-PCR results showing inhibition of RCBTB1 by shRNA. SW872 and LPS141 cells were transduced with either scrambled control (SCR) or shRCBTB1 vectors (SH1 and SH2), and stable clones were selected by puromycin. (**e**) Apoptosis assay results of LPS141 cells shown as a representative image. (**f**) Summary of apoptosis assay results. Stable clones were exposed to apoptotic stress (nocodazole) for 48 h and subjected to FACS analysis. Data represent average ± s.d. (error bars). Asterisk (*) indicatse *P*-value <0.05 by *t*-test.

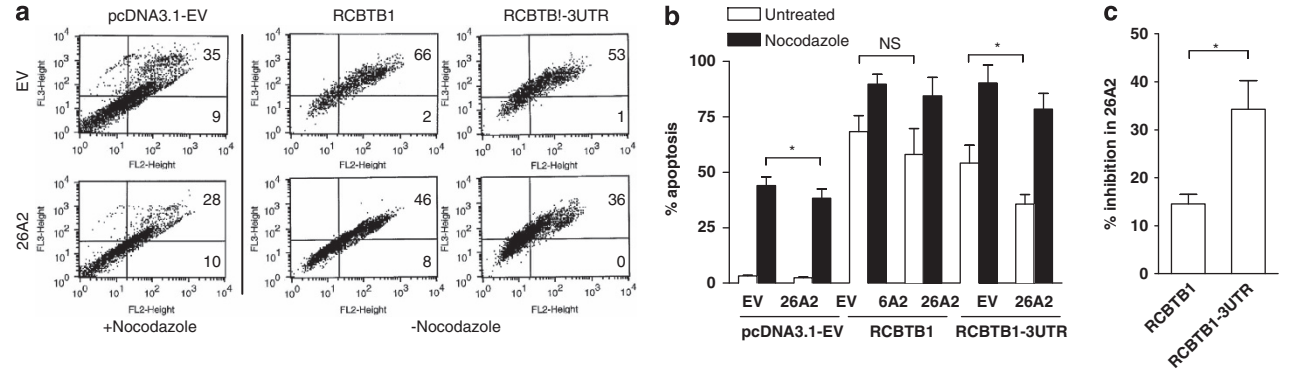

Figure 7. Effect of miR-26a-2 on RCBTB1-induced apoptosis. Cotransfection of miR-26a-2 with either RCBTB1 (no 3′-UTR) or RCBTB1-3UTR (having 3′-UTR miR-26a-2-binding site) expression vector in SW872 cells using the same conditions as in Figure 6. (**a**) Selected image of the apoptosis assay results. (**b**) Summary of the apoptosis assay results (**c**) Summary of the effect of miR-26a-2 on the inhibition of RCBTB1-induced apoptotis. Data represents average ± s.d. (error bars). Asterisk (*) indicates *P*-value <0.05 by *t*-test.

purchased from the Tumor Repository at Yale University School of Medicine (New Haven, CT, USA). Twenty-eight samples (LPS25–LPS52) were obtained from Dr Lawrence M Weiss at City of Hope (Duarte, CA, USA). Twenty-one samples (LPS53–LPS75) were from Dr Eng Chon Boon at the NUHS Tissue Repository of the National University of Singapore (NUS, Singapore). Three DNA samples (LPS10, LPS56 and LPS60) were partially degraded and have been excluded from the study.

Thirteen matched and non-matched normal fat tissues were also obtained (Supplementary Table S4). Five non-matched normal fat tissues (F1–F5) were provided by Dr Jonathan Said. Six samples (LPS11, 12, 13, 15,

19 and 22) obtained from the Yale tumor repository had matched normal fat tissues from the same patients. They were subjected to paired analysis. Two samples (LPS55 and LPS60) were from NUS, which had matched normal samples.

Human LPS cell lines

Three human LPS cell lines (SW872, LPS141 and LP6) were included in the study: SW872 cells were purchased from American Tissue Type Culture Collection (ATCC, Rockville, MD, USA); LPS141 and LP6 cells were provided by Dr Christopher DM Fletcher at Brigham and Women's Hospital (Boston, MA, USA).[22] All three LPS cell lines were maintained in RPMI medium (Mediatech Inc, Herndon, VA, USA) supplemented with 15% fetal bovine serum (Atlanta Biological, Lawrenceville, GA, USA) in a humidified incubator at 37 °C supplied with 5% CO_2. Only cells in the exponential growth phase were used in the study.

SNP array analysis

SNP array analysis was performed using GeneChip human mapping SNP array (Affymetrix, Santa Clara, CA, USA). Briefly, genomic DNA from 75 human LPS samples were purified using DNeasy DNA purification kit according to the manufacturer's protocol (Qiagen, Valencia, CA, USA) and hybridized to Affymetrix 250K NspI SNP array. GeneChip Fluidics Station 400 and GeneChip scanner 3000 were used to produce raw data, which were processed and analyzed by CN analyzer for Affymetrix GeneChip (CNAG 2.0) using allele-specific CN analysis, employing anonymous reference (AsCNAR) algorithm.[18]

Quantitative reverse-transcription real-time PCR

Total RNAs from all LPS samples were purified using miRNeasy RNA purification kit according to the manufacturer's protocol (Qiagen). First-strand cDNA was made using iScript cDNA construction kit according to the manufacturer's protocol (Bio-Rad, Hercules, CA, USA). qRT-PCR was performed with Bio-Rad SsoFast EvaGreen Supermix in Bio-Rad CFX96 PCR detection system (Bio-Rad). Primer pairs used in this study were listed in Supplementary Table S5. The relative expression level of each gene was normalized to the GAPDH expression level of each sample by $\Delta\Delta C_t$ method.

Modulation of miR-26a-2 expression level in LPS cell lines

The effect of overexpression of miR-26a-2 was examined in SW872 and LPS141 cell lines using pMSCV retroviral expression vector. Briefly, 460 bp genomic region containing miR-26a-2 coding sequence was amplified by PCR using the primer set in the Supplementary Table S5. The PCR product was ligated into the pMSCV vector using *Bgl*II and *Eco*RI.

Retroviral packaging was performed in 293T cells by cotransfecting pMSCV-miR-26a-2 vector with packaging vectors pCMV-Gag-Pol and RD114 envelope vector using Profection mammalian transfection system, according to the manufacturer's protocol (Promega, Madison, WI, USA). LPS cell lines were infected with viral supernatant containing either miR-26a-2 expression vector or empty vector control with 4 μg/ml polybrene solution. After 48 h, stable clones were selected using puromycin. The overexpression of miR-26a-2 was validated by qRT-PCR.

The effect of inhibition of miR-26a-2 was examined in LPS141 and LP6 cell lines using miScript anti-hsa-miR-26a-2* miRNA inhibitor oligos and the control siRNA oligs (Qiagen). LP141 and LP6 cells were transfected with the oligos at a concentration of 50 nM using jetPRIME siRNA transfection reagent, according to the manufacturer's protocol (BIOPARC, Illkirch, France). After 24 h, the inhibition of miR-26a-2 was validated by qRT-PCR.

Luciferase reporter assay

pGL3-promoter vector containing the miR-26a-2-binding site in 3′-UTR region of the *RCBTB1* gene was constructed using primer sets shown in Supplementary Table S5. To introduce point mutations to the miR-26a-2-binding site, Quikchange II XL site-directed mutagenesis kit was used, according to the manufacturer's protocol (Stratagene, La Jolla, CA, USA). Cotransfection of pGL3-Promoter-RCBTB1 3′-UTR vector and pRL-TK renilla luciferase vector, along with either miR-26a-2 expression vector or empty vector control, was performed using Bio-T transfection reagent according to the manufacturer's protocol (BioLand LLC, Paramount, CA). After 48 h, cells were harvested and subjected to dual luciferase assay using Promega dual luciferase reporter assay kit according to the manufacturer's protocol.

Modulation of RCBTB1 expression level in LPS cell lines

For overexpression of *RCBTB1* gene, pCMT-RCBTB1-HA-tag expression vector was obtained from Dr Xiaobo Zhou.[16] LPS141 and LP6 cells were transfected with either RCBTB1 expression vector or empty vector control using jetPRIME DNA transfection reagent according to the manufacturer's protocol (BIOPARC). Subsequent experiments were performed after 48 h of incubation. Expression of RCBTB1 was validated by qRT-PCR and western blot.

For inhibition studies, pLKO.1-shRCBTB1 lentiviral vectors were constructed using the primer sets, as shown in Supplementary Table S5. The pLKO.1-scrambled shRNA-negative control vector (Addgene plasmid 1864) was obtained from Addgene (Cambridge, MA, USA).[23] Lentiviral packaging was performed in 293T cells by cotransfecting pLKO.1-shRCBTB1 vectors with packaging vectors pCMV-Gag-Pol, pRev and RD114 envelope vector, using Profection mammalian transfection system according to the manufacturer's protocol (Promega). LPS cell lines were infected with viral supernatants of either shRCBTB1 vector or scrambled shRNA vector control, with 4 μg/ml polybrene solution. After 48 h, stable clones were selected using puromycin. The inhibition of RCBTB1 was validated by qRT-PCR and western blot.

Western blotting

Western blotting was performed as described previously.[24] Primary antibodies used in the study are listed in Supplementary Table S6.

Cell growth and proliferation assays

Cell growth was measured by 3-(4,5-dimethylthiazol-2-yl)-2,5-diphenyltetrazolium bromide (MTT) assay (Sigma-Aldrich, St Louis, MO, USA), as described previously.[24] Clonogenic ability of the LPS cells was monitored by soft agar colony-formation assay. A 0.8% base layer was made in 24-well plates, followed by a 0.7% top layer containing the cell suspension. After 2–3 weeks of incubation, colonies were counted using a dissecting microscope.

Cell migration assays

For the wound-healing assay, cells were seeded in six-well plates and incubated until confluence. Scratches were made on the cell monolayer, and pictures were taken at regular time intervals up to 24 h. ImageJ was used to measure the gap width.[25] For Boyden chamber assay, cells were cultured in serum-free RPMI media for 48 h prior to harvesting. Boyden chamber was made by placing cell culture inserts in 24-well plates (8.0-μm pore size) (BD Biosciences, San Jose, CA, USA). Cells were seeded in the upper layer of the chamber in serum-free RPMI media, and bottom chamber was filled with RPMI media with 15% fetal bovine serum. After 12 h, cells that had migrated through the membrane were counted after crystal violet staining.

Cell cycle analysis and apoptosis assay

Cell cycle analysis and apoptosis assay were carried out as described previously.[24] For cell cycle analysis, cells were exposed to 0.1 μg/ml nocodazole for 16 h (Sigma-Aldrich). For apoptosis assay, cells were exposed to 0.5 μg/ml nocodazole for 72 h.

In vitro adipocyte differentiation assay

Primer pairs of the adipocyte differentiation marker genes for qRT-PCR were described by Mariani *et al.*[26]

Statistical analysis

For all statistical tests, *P*-value $\leqslant 0.05$ was considered statistically significant and marked by a single asterisk (*). *P*-value less than or equal to 0.001 were marked by double asterisks (**). Two-tailed Student's *t*-test with unequal variances was used to compare the difference between two experimental groups. All experiments were repeated at least three times to ensure accuracy. χ^2 test was used to determine if the occurrence of two different CN change events was associated or independent. Pearson's correlation test was used to measure the correlation between the two groups. Correlation coefficient of 0.5 or higher was considered significant at the 0.05 level. Patients with survival data were subjected to Kaplan–Meier survival analysis using GraphPad Prism 4.0 (GraphPad Software Inc, La Jolla, CA).

CONFLICT OF INTEREST

The authors declare no conflict of interest.

ACKNOWLEDGEMENTS

This research has been funded by the Sarcoma Foundation of America. H.P.K received Grant support from NIH R0-1 CA026038-38 and U54-14 39 30, as well as A* STAR Grant of Singapore.

REFERENCES

1 Conyers R, Young S, Thomas DM. Liposarcoma: molecular genetics and therapeutics. *Sarcoma* 2011; **2011**: 483154.
2 Crago AM, Singer S. Clinical and molecular approaches to well differentiated and dedifferentiated liposarcoma. *Curr Opin Oncol* 2011; **23**: 373–378.
3 Müller CR, Paulsen EB, Noordhuis P, Pedeutour F, Saeter G, Myklebost O. Potential for treatment of liposarcomas with the MDM2 antagonist Nutlin-3A. *Int J Cancer* 2007; **121**: 199–205.
4 Singer S, Socci ND, Ambrosini G, Sambol E, Decarolis P, Wu Y *et al.* Gene expression profiling of liposarcoma identifies distinct biological types/subtypes and potential therapeutic targets in well-differentiated and dedifferentiated liposarcoma. *Cancer Res* 2007; **67**: 6626–6636.
5 Garofalo M, Croce CM. microRNAs: master regulators as potential therapeutics in cancer. *Annu Rev Pharmacol Toxicol* 2011; **51**: 25–43.
6 Huse JT, Brennan C, Hambardzumyan D, Wee B, Pena J, Rouhanifard SH *et al.* The PTEN-regulating microRNA miR-26a is amplified in high-grade glioma and facilitates gliomagenesis *in vivo*. *Genes Dev* 2009; **23**: 1327–1337.
7 Kim H, Huang W, Jiang X, Pennicooke B, Park PJ, Johnson MD. Integrative genome analysis reveals an oncomir/oncogene cluster regulating glioblastoma survivorship. *Proc Natl Acad Sci USA* 2010; **107**: 2183–2188.
8 Rieker RJ, Weitz J, Lehner B, Egerer G, Mueller A, Kasper B *et al.* Genomic profiling reveals subsets of dedifferentiated liposarcoma to follow separate molecular pathways. *Virchows Arch* 2010; **456**: 277–285.
9 Italiano A, Bianchini L, Keslair F, Bonnafous S, Cardot-Leccia N, Coindre JM *et al.* HMGA2 is the partner of MDM2 in well-differentiated and dedifferentiated liposarcomas whereas CDK4 belongs to a distinct inconsistent amplicon. *Int J Cancer* 2008; **122**: 2233–2241.
10 Sanada M, Suzuki T, Shih L, Otsu M, Kato M, Yamazaki S *et al.* Gain-of-function of mutated C-CBL tumour suppressor in myeloid neoplasms. *Nature* 2009; **460**: 904–908.
11 Betel D, Wilson M, Gabow A, Marks DS, Sander C. The microRNA.org resource: targets and expression. *Nucleic Acids Res* 2008; **36**: D149–D153.
12 Dweep H, Sticht C, Pandey P, Gretz N. miRWalk--database: prediction of possible miRNA binding sites by 'walking' the genes of three genomes. *J Biomed Inform* 2011; **44**: 839–847.
13 Griffiths-Jones S, Saini HK, van Dongen S, Enright AJ. miRBase: tools for microRNA genomics. *Nucleic Acids Res* 2008; **36**: D154–D158.
14 Krek A, Grün D, Poy MN, Wolf R, Rosenberg L, Epstein EJ *et al.* Combinatorial microRNA target predictions. *Nat Genet* 2005; **37**: 495–500.
15 Lewis BP, Burge CB, Bartel DP. Conserved seed pairing, often flanked by adenosines, indicates that thousands of human genes are microRNA targets. *Cell* 2005; **120**: 15–20.
16 Zhou X, Münger K. Clld7, a candidate tumor suppressor on chromosome 13q14, regulates pathways of DNA damage/repair and apoptosis. *Cancer Res* 2010; **70**: 9434–9443.
17 Calin G, Dumitru C, Shimizu M, Bichi R, Zupo S, Noch E *et al.* Frequent deletions and down-regulation of micro- RNA genes miR15 and miR16 at 13q14 in chronic lymphocytic leukemia. *Proc Natl Acad Sci USA* 2002; **99**: 15524–15529.
18 Nannya Y, Sanada M, Nakazaki K, Hosoya N, Wang L, Hangaishi A *et al.* A robust algorithm for copy number detection using high-density oligonucleotide single nucleotide polymorphism genotyping arrays. *Cancer Res* 2005; **65**: 6071–6079.
19 Barretina J, Taylor BS, Banerji S, Ramos AH, Lagos-Quintana M, Decarolis PL *et al.* Subtype-specific genomic alterations define new targets for soft-tissue sarcoma therapy. *Nat Genet* 2010; **42**: 715–721.
20 Mabuchi H, Fujii H, Calin G, Alder H, Negrini M, Rassenti L *et al.* Cloning and characterization of CLLD6, CLLD7, and CLLD8, novel candidate genes for leukemogenesis at chromosome 13q14, a region commonly deleted in B-cell chronic lymphocytic leukemia. *Cancer Res* 2001; **61**: 2870–2877.
21 Rual JF, Venkatesan K, Hao T, Hirozane-Kishikawa T, Dricot A, Li N *et al.* Towards a proteome-scale map of the human protein-protein interaction network. *Nature* 2005; **437**: 1173–1178.
22 Snyder EL, Sandstrom DJ, Law K, Fiore C, Sicinska E, Brito J *et al.* c-Jun amplification and overexpression are oncogenic in liposarcoma but not always sufficient to inhibit the adipocytic differentiation programme. *J Pathol* 2009; **218**: 292–300.
23 Sarbassov DD, Guertin DA, Ali SM, Sabatini DM. Phosphorylation and regulation of Akt/PKB by the rictor-mTOR complex. *Science* 2005; **307**: 1098–1101.
24 Lee DH, Thoennissen NH, Goff C, Iwanski GB, Forscher C, Doan NB *et al.* Synergistic effect of low-dose cucurbitacin B and low-dose methotrexate for treatment of human osteosarcoma. *Cancer Lett* 2011; **306**: 161–170.
25 Abramoff MDM, Magalhaes PJ, Ram SJ. Image processing with ImageJ. *Biophotonics Int* 2004; **11**: 36–42.
26 Mariani O, Brennetot C, Coindre JM, Gruel N, Ganem C, Delattre O *et al.* JUN oncogene amplification and overexpression block adipocytic differentiation in highly aggressive sarcomas. *Cancer Cell* 2007; **11**: 361–374.

Supplementary Information accompanies this paper on the Oncogenesis website (http://www.nature.com/oncsis).